

EFFECT OF La AND Ce CO-DOPING ON STRUCTURAL, SPECTRAL AND ELECTRICAL PROPERTIES OF Ba-Ni M TYPE HEXAFERRITES

M. RAMZAN^a, M. I. ARSHAD^a, N. AMIN^a, K. MAHMOOD^a, A. ALI^a, M. SHARIF^a, S. IKRAM^a, Y. JAMIL^b, M. AJAZ-UN-NABI^{a,*}

^a*Department of Physics, Government College University Faisalabad 38000, Pakistan*

^b*Department of Physics, Agriculture University, Faisalabad 38000, Pakistan*

In this study, a series of $\text{Ba}_{0.8}\text{Ni}_{0.2}\text{Fe}_{(12-y-x)}\text{Ce}_x\text{La}_y\text{O}_{19}$ ($0 \leq x, y \leq 0.3$) hexaferrites was prepared by sol gel auto combustion method. The XRD was used for the structural analysis of prepared samples. The obtained XRD patterns confirmed the formation of M-type hexaferrites and the average crystallite size of the prepared samples was found in the range 19.51 to 32.58 nm. The electrical properties were investigated by two probe technique. It was revealed that the electrical resistivity of sample with La content is higher than that of the samples without La content. The maximum resistivity was found for the sample with $x = 0.3, y = 0.3$. The UV-vis results exhibit that the bandgap of the samples was increased with the inclusion of La and increases with the increase in La content.

(Received May 22, 2019; Accepted Accepted September 25, 2019)

Keywords: M-type Hexagonal Ferrites, Sol-gel Auto combustion, Rare-earth, Optical bandgap, Electrical resistivity

1. Introduction

Radars are used to detect and locate objects (like aero-planes, missiles) and radio or microwave domains are used for these purposes. To deceive these radars, microwave absorbers are used in the missiles and aero-planes these days. Hexagonal ferrites due to their high natural resonance frequency and large saturation magnetization are one of the major constituents of the microwave absorber material used for these stealth purposes [1, 2]. For ferrites to be used in electrical and dielectric applications, high magnetic permeability, electrical resistivity, coercivity and low hysteresis loss are required. Similarly, intermediate coercivity and high saturation magnetization and energy product $(\text{BH})_{\text{max}}$ are needed for data storage and tape media recording purposes [3]. To enhance the properties of the pure BaM different techniques are used such as preparation methods (co-precipitation, sol-gel, sol-gel auto-combustion, ceramic method etc.) and ions substitution (di-valent, tri-valent or tetravalent). In present work we substitute Ni^{2+} and Ce^{3+} cations to change the properties of pure BaM due to their similarity in ionic radii and electronic configurations, where Ni^{2+} is a ferromagnetic element and it was reported that it's substitution in a small amount could increase the grain size, transmittivity and photoconductivity, electrical conductivity (by increasing the hole in the material, p-type) and reduce the coercivity remarkably [4, 5, 6, 7]. The literature also shows that Ni is beneficial for the environment and organism, cheap and steady and at the same time it would scarcely influence the structure of the crystal [7]. Due to its high electrical resistivity Re^{3+} ions substitution increases the electrical resistivity of the ferrites that is important for the devices to operate at high frequencies [3, 8, 9, 10]. In this study, a systematic attempt has been made to investigate the structural, optical and electrical properties of the BaM ferrites containing Ni^{2+} and Ce^{3+} and La^{3+} .

*Corresponding author: majazunnabi@gcuf.edu.pk

2. Experimental

$Ba_{0.8}Ni_{0.2}Fe_{(12-y-x)}Ce_xLa_yO_{19}$ ($0 \leq x, y \leq 0.3$) were prepared by sol gel auto combustion method. Research grade $BaCl_2 \cdot 2H_2O$, $Ni(NO_3)_2 \cdot 6H_2O$, $Fe(NO_3)_3 \cdot 9H_2O$, $La(NO_3)_3 \cdot xH_2O$, $Ce(NO_3)_3 \cdot 6H_2O$, citric acid ($C_6H_8O_7 \cdot H_2O$) and NH_4OH were used as the starting material. Stoichiometric amount of all chemicals was mixed one by one separately in small amount of water and stirred at $75^\circ C$ for 15 minutes then mixed all solutions in single beaker to form a homogeneous solution and added citric acid $C_6H_8O_7 \cdot H_2O$ with molar ratio 1:2 in solution and stirred for 30 minutes maintaining a temperature of 90 to $95^\circ C$, as among all other fuels citric acid has low ignition temperature (i.e. $200-250^\circ C$) and better complexing ability.

The reaction was controlled by nitrates and NH_4OH was added drop by drop to maintain the pH of the solution between 7 to 8. The solution was dehydrated at 150 to $180^\circ C$ until a dry gel was formed, continuing stirring finally ignited the gel by increasing the temperature up to 260 to $275^\circ C$. A loose powder was formed at this stage. Finally, calcined the powder at $1200^\circ C$ at gradual temperatures $500^\circ C$ (30 min), $700^\circ C$ (30 min), $900^\circ C$ (30 min), $1100^\circ C$ (30 min) and $1200^\circ C$ (2- hour) and cool down the samples slowly and steadily up to room temperature to form hexa-ferrite phase.

For I-V analysis made the circular pellets of the samples using polyvinyl alcohol as a binder at 5tons ($D = 1.4254$ cm and thickness 0.4210 cm) for 1-2 minutes.

The X-ray diffraction (XRD) technique was used to study the crystal structure of the prepared samples and bond formation was studied by FTIR. Bandgap variations were found by using UV-Visible Spectroscopy. The dc electrical resistivity was determined by home made two-probe method.

3. Results and discussion

3.1. XRD analysis

The X-ray diffraction patterns of the as prepared non-substituted and substituted samples calcined at $1200^\circ C$ have been presented in Fig. 1. The observed peaks for BaM were identified by comparing with the JCPDS cards (COD 9012763, COD 1009038 and space group $P6_3/mmc$). From the patterns, it is clear that the major crystalline phase is M-type hexagonal and there is no other phase appearing in the pattern [1, 11]. The Fig. 2 shows that the max. and min. average grain size of as prepared powder is found 32.58 nm and 19.51 nm respectively by Scherrer's formula:

$$D = \frac{k\lambda}{\beta_{hkl} \cos \theta} \quad (1)$$

The lattice parameters a and c were calculated by the value of d_{hkl} corresponding to (1 0 7) and (1 1 4) by using the following equation:

$$\frac{1}{d^2_{hkl}} = \frac{4}{3} \left(\frac{h^2 + k^2 + l^2}{a^2} \right) + \frac{l^2}{c^2} \quad (2)$$

The average x-ray density was measured by using formula

$$D_{X-Ray} = \frac{ZM}{N_{AV}} \quad (3)$$

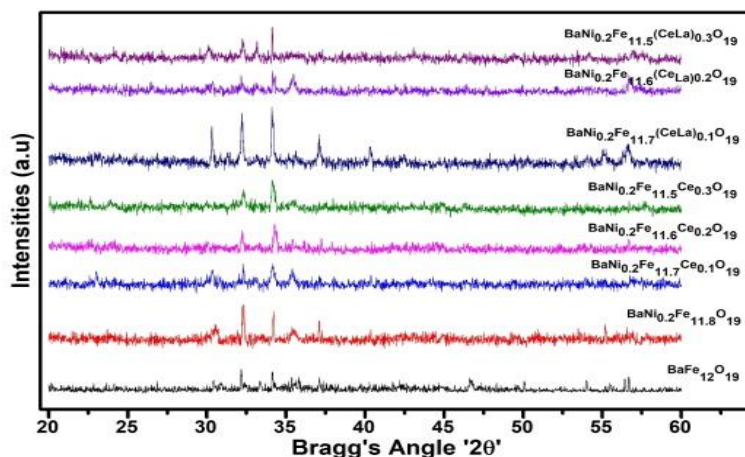


Fig. 1. X-ray diffraction patterns for $Ba_{0.8}Ni_{0.2}Fe_{(12-y-x)}Ce_xLa_yO_{19}$ ($0 \leq x, y \leq 0.3$) ferrites.

Table 1. Lattice parameters, Crystallite size, X-ray density, d-values of the $BaNi_yFe_{(12-y-x)}Re_xO_{19}$ ($0 \leq x \leq 0.3, y = 0.2$) ferrites.

Composition (x)	A	c	crystallite size	Unit Cell Volume	X-Ray Density	d-values
		Å	Nm	(Å) ³	g/cm ³	Å
Ni=0	5.89	23.274	32.58	700.298	5.198	2.628
Ni=0.2	5.89	23.209	32.46	693.874	5.246	2.626
Ce=0.1	5.89	23.274	22.44	699.229	5.206	2.628
Ce=0.2	5.89	23.145	23.89	691.946	5.261	2.625
Ce=0.3	5.89	23.170	24.52	692.717	5.255	2.625
CeLa=0.1	5.89	23.209	19.51	693.874	5.246	2.626
CeLa=0.2	5.89	23.213	21.59	694.003	5.245	2.626
CeLa=0.3	5.89	23.188	23.06	693.231	5.251	2.626

3.2. Optical measurements

The samples for UV-Vis analysis were prepared by mixing powder in de-ionized water as suspension and the obtained spectra were used to calculate the optical bandgap (E_g) of prepared hexaferrites. The UV-vis spectroscopy measurements were made at room temperature in the wavelength range 200 – 1100 nm using the Perkin Elmer UV Win Lab Data Processor.

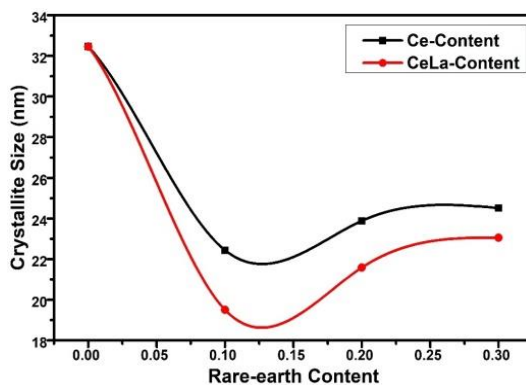


Fig. 2. Crystallite Size vs rare-earth content of $Ba_{0.8}Ni_{0.2}Fe_{(12-y-x)}Ce_xLa_yO_{19}$ ($0 \leq x, y \leq 0.3$) ferrites.

The optical bandgap E_g was calculated using the following equation:

$$\alpha hv = A (hv - E_g)^n \quad (3)$$

where ‘A’ and ‘ α ’ represent a constant and absorption coefficient respectively, whereas ‘n’ exhibits value of 1/2 and 2 for direct and indirect bandgap materials, respectively.

The plots of $(\alpha hv)^2$ versus hv shown in Fig. 3 (a, b and c) are called Tauc graphs. The optical bandgaps (E_g) were determined using the intercept of the Tauc plot at $\alpha = 0$ [12]. Fig. 4 displays the optical bandgap of our samples as a function of rare-earth cation’s content. It can be seen from Fig. 4 that E_g decreases first for $x = 0$ to $x = 0.1$ and almost linearly increased for $x = 0.1$ to $x = 0.3$. The value of E_g varies between minimum 2.50 eV (belongs to $\text{BaNi}_{0.2}\text{Fe}_{11.7}\text{Ce}_{0.1}\text{O}_{19}$ hexaferrite) and maximum 3.21 eV (belongs to $\text{BaNi}_{0.2}\text{Fe}_{11.8}\text{O}_{19}$ hexaferrite). It is evident from the literature that our samples exhibit decreased band gap that is suitable for optical applications in the solar spectrum range. The reported values for optical bandgap of hexaferrites lie in the range of 3.18 – 3.92 eV [13, 14].

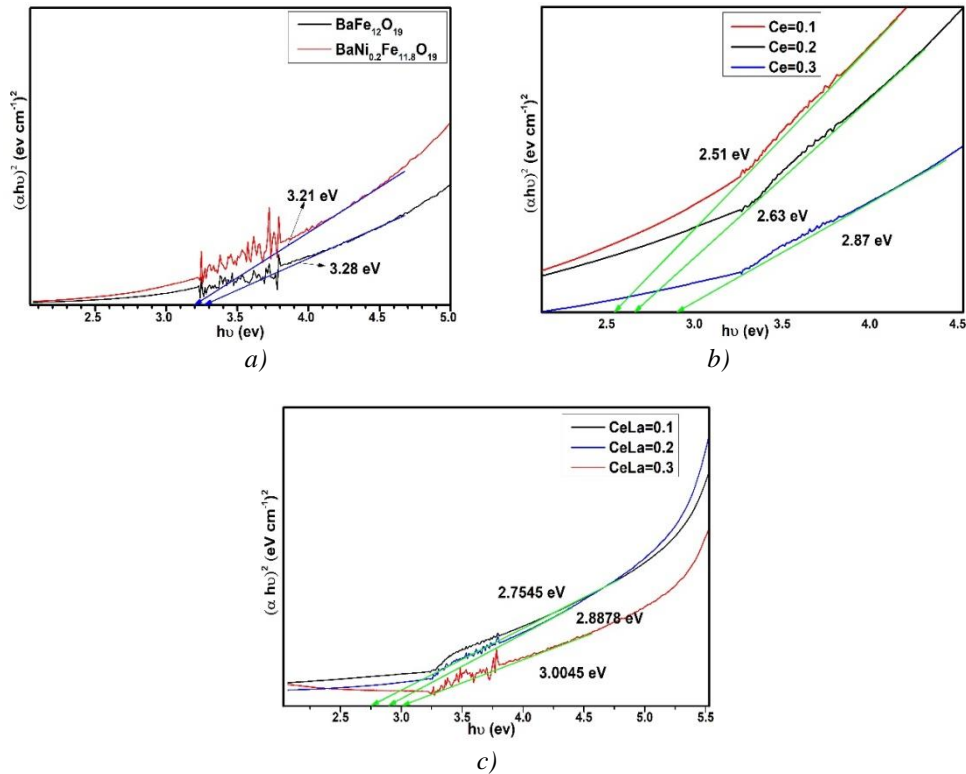


Fig. 3. UV-Vis spectra for $\text{BaNi}_y\text{Fe}_{(12-y-x)}\text{Re}_x\text{O}_{19}$ ($0 \leq x \leq 0.3$, $y = 0.2$) ferrites. (a) pure and Ni-substituted (b) Ce-substituted (c) CeLa-substituted.

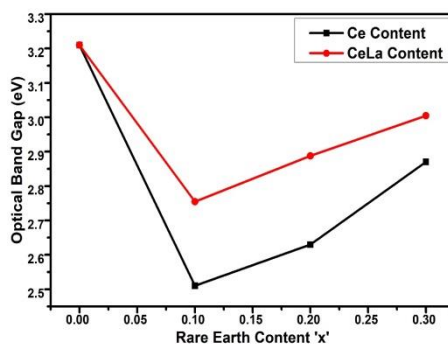


Fig. 4. Optical band gap vs Rare-earth Content for $BaNi_yFe_{(12-y-x)}Re_xO_{19}$ ($0 \leq x \leq 0.3$, $y = 0.2$) ferrites.

3.3. Electrical measurements

The resistivity and activation energies are measured at temperature 473 K as shown in Fig. 5. The resistivity increases from a value 3.424×10^8 to $3.024 \times 10^9 \Omega\text{ cm}$ for Ce-content and $6.26 \times 10^8 \Omega\text{ cm}$ to $4.0717 \times 10^9 \Omega\text{ cm}$ for CeLa-content with increasing rare-earth concentration [10]. The increase in resistivity may be due to the limit of hopping probability of electrons between Fe^{3+} and Fe^{2+} ions, as rare earth ions prefer to occupy octahedral sites in hexagonal structure. It may force the Fe^{3+} ions to migrate from octahedral sites to tetrahedral sites to compensate the overall neutrality. As a consequence of this migration, the concentration of Fe^{3+} ions is reduced at octahedral sites which are responsible for conduction in ferrites. The above discussed phenomena are the possible reasons for increase in dc electrical resistivity. [15, 16, 17, 18, 19]

The value of activation energy also increases with increase of rare-earth content from 0.4647 eV to 0.5547 eV for Ce-content and 0.4647 eV to 0.5666 eV for CeLa-content. It may be assumed that due to increase in resistivity with the increase of rare-earth content, as activation energy behaves in the same way as electrical resistivity. [16]

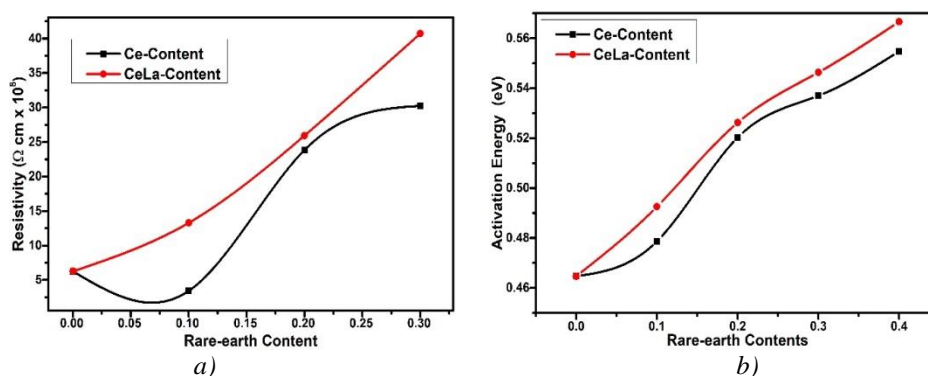


Fig. 5. (a) Resistivity and (b) Activation Energy vs Rare-earth Content for $Ba_{0.8}Ni_{0.2}Fe_{(12-y-x)}Ce_xLa_yO_{19}$ ($0 \leq x, y \leq 0.3$) ferrites at 473 K .

3. Conclusions

The M-type hexagonal nano-ferrites having general formula $BaNi_yFe_{(12-x-y)}Re_xO_{19}$ doped with Re^{3+} ions, were successfully prepared by the standard sol-gel auto combustion method. The XRD analysis confirmed the single phase of synthesized nano-particles. The optical bandgap determined by UV-vis spectroscopy ranges from 2.50 to 3.21 eV . Electrical resistivity was observed to be decreases with increase in temperature and it confirmed the semiconducting nature of ferrites. The activation energy E_g of the prepared samples was observed to be increased from

0.46 to 0.57 eV with increase in Re-content and this increase is due to reduced electron super-exchange between Fe^{2+} and Fe^{3+} ions. The obtained characteristics are important for reduction in eddy current losses in hexagonal ferrites. These results suggest that the investigated ferrites are potential candidates for applications in high frequency range, radar wave absorbing materials and for electromagnetic interference attenuation.

References

- [1] Sun Chang, SunKangning, ChuiPengfei, *Journal of Magnetism and Magnetic Materials* **324**, 802 (2012).
- [2] Widyastuti, Nia Sasria, A Marsha Alviani, M Dwi Febri R and Vania Mitha., *IOP Conf. Series: Journal of Physics: Conf. Series*, no. 012015, p. 877, 2017.
- [3] Goldman, Alex, second edition ed., Springer Science & Business Media, 2006, pp. 219-220.
- [4] S. Kanagesan, S. Jesurani, R. Velmurugan, *J Mater Sci: Mater Electron.* **23**, 952 (2012).
- [5] Taminder Singh, M S Batra, Iqbal Singh and Arun Katoch., *Journal of Physics: Conference Series* 534 (2014) 012013, no. 012013, p. 534, 2014.
- [6] Ankush Thakur, R.R.Singh, P.B.Barman., *Journal of Magnetism and Magnetic Materials* **326**, 35 (2013).
- [7] Jiaqi Pan, ShikuanGuo, XinZhang, BoxueFeng, WeiLan, "The photoconductivity properties of transparent Ni-doped CuAlO_2 films," *Materials Letters* **96**, 31 (2013).
- [8] wikipedia, google, 01 2019. [Online]. Available: <https://en.wikipedia.org/wiki/Cerium>. [Accessed 01-january-2019].
- [9] Mukhtar Ahmad, Faiza Aen, M.U. Islam, Shahida B. Niazi, M.U. Rana, *Ceramics International* **37**, 3691 (2011).
- [10] Muhammad F. Din, Ishtiaq Ahmad, Mukhtar Ahmad, M.T. Farid, M. Asif Iqbal, G. Murtaza, Majid Niaz Akhtar, Imran Shakir, Muhammad Farooq Warsi, Muhammad Azhar Khan, *Journal of Alloys and Compounds.* **584**, 646 (2014).
- [11] Li Jie, Zhang Huaiwu, Li Qiang, Li Yuanxun, Yu Guoliang, *Journal of Rare Earths* **31**, Oct. 983 (2013).
- [12] K. Alamelu Mangai, K. Tamizh Selvi, M. Priya, M. Rathnakumari, P. Sureshkumar, Suresh Sagadevan, *Journal of Material Science: Mater Electron.* **28**, 1238 (2017).
- [13] I. A. Auwal, A. Baykal, S. Güner, M. Sertkol, H. Sözeri, *Journal of Magnetism and Magnetic Materials* **409**, 92 (2016).
- [14] S. Güner, I. A. Auwal, A. Baykal, H. Sözeri, *Journal of Magnetism and Magnetic Materials*, **416**, 261 (2016).
- [15] Mukhtar Ahmad, Faiza Aen, M.U. Islam, Shahida B. Niazi, M.U. Rana, *Ceramics International* **37**, 3691 (2011).
- [16] M. Raghasudha, D. Ravinder, P. Veerasomaiah, *Materials Discovery* **2**, 50 (2015).
- [17] Pradeep Chavan, L.R. Naik, P.B. Belavi, Geeta Chavan, C.K. Ramesha, and R.K. Kotnala, *Journal of Electronic Materials* **46**(1), 188 (2017).
- [18] B. S. Satone, K. G. Rewatkar, *International Journal of Current Trends in Engineering & Research (IJCTER)* **2**(4), 74 (2016).
- [19] D. Ravinder, P. Shalini, P. Mahesh, K. Koteswara Rao, M. Vithal, B. S. Boyanov, *Journal of Alloys and Compounds.* **364**, 17 (2004).